Acta Cryst E CRYSTALLOGRAPHIC COMMUNICATIONS

ISSN 2056-9890

An orthorhombic polymorph of isavuconazole

Anna Ben[a,b]* and Lilianna Chęcińska[b]

[a]University of Lodz Doctoral School of Exact and Natural Sciences, Narutowicza 68, 90-136 Łódź, Poland, and [b]University of Lodz, Faculty of Chemistry, Pomorska 163/165, 90-236 Łódź, Poland. *Correspondence e-mail: anna.ben@edu.uni.lodz.pl

Received 10 October 2025
Accepted 13 October 2025

Edited by L. Van Meervelt, Katholieke Universiteit Leuven, Belgium

Keywords: isavuconazole; crystal structure; polymorph; energy frameworks.

CCDC reference: 2495049

Supporting information: this article has supporting information at journals.iucr.org/e

The title compound $C_{22}H_{17}F_2N_5OS$ (systematic name: 4-{2-[(2*R*,3*R*)-3-(2,5-difluorophenyl)-3-hydroxy-4-(1,2,4-triazol-1-yl)butan-2-yl]-1,3-thiazol-4-yl}benzonitrile), represents a new orthorhombic polymorph of isavuconazole. The two stereogenic centers adopt the *R*,*R* configuration. In the crystal structure of the orthorhombic form, a mono-periodic chain motif is formed by a strong O—H···N hydrogen bond, while three additional C—H···N interactions propagate these chains into a tri-periodic supramolecular network. A comparison with the previously reported monoclinic polymorph [Voronin *et al.* (2021). *CrystEngComm* **23**, 8513] is provided, supported by Hirshfeld surface and energy framework analyses.

1. Chemical context

Heterocyclic compounds have long attracted considerable attention due to their importance as structural intermediates in many biologically active substances (Raman *et al.*, 2025). For over a century, they have been one of the key areas of research in organic chemistry. Nitrogen-containing heterocycles, in particular, exhibit a wide range of applications, from pharmaceuticals and agriculture, through materials science and coordination chemistry, to the dye and pigment industry (Salma *et al.*, 2024). Among these, triazole derivatives have drawn significant interest in recent decades due to their diverse chemical and biological activities, including antifungal (Li *et al.*, 2019), anticancer (Slaihim *et al.*, 2019), and antibacterial properties (Hussain *et al.*, 2019).

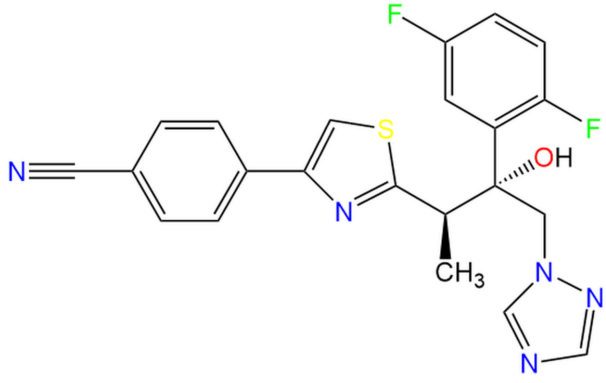

Isavuconazole is a novel and promising broad-spectrum triazole used to treat invasive fungal infections in humans (Shirley & Scott, 2016). This drug is available in both intravenous and oral formulations (Lewis II *et al.*, 2022) and demonstrates activity against yeasts, molds, and dimorphic fungi. Moreover, it has been approved for the treatment of invasive aspergillosis and mucormycosis (Miceli & Kauffman, 2015).

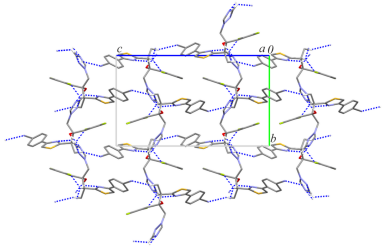

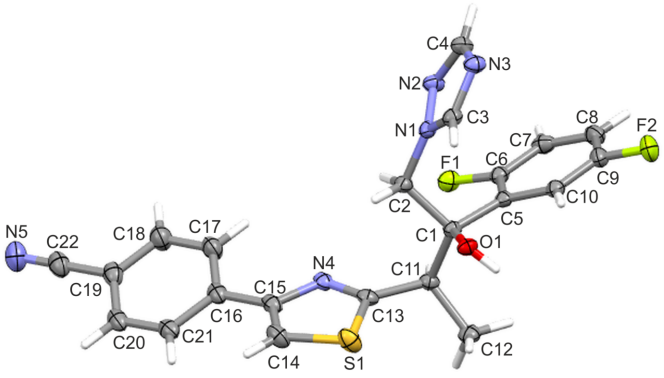

Figure 1
The molecular structure of ISV-ortho with the atom-numbering scheme. Displacement ellipsoids are drawn at the 50% probability level and H atoms are shown as small spheres of arbitrary radii.

Only four crystal structures of isavuconazole have been reported to date: the pure form, a monohydrate, and two salts (Voronin *et al.*, 2021). In this article a crystal structure of a new orthorhombic form of pure isavuconazole (ISV-ortho) is reported, and compared with its monoclinic form (ISV-mono) (Voronin *et al.*, 2021).

2. Structural commentary

The title compound is orthorhombic, crystallizing in space group $P2_12_12_1$. The molecule (Fig. 1) consists of four rings (1,2,4-triazole, 2,5-difluorophenyl, 1,3-thiazole and benzonitrile) and a hydroxyl group connected to each other by a flexible chain. In both polymorphs of isavuconazole, ISV-ortho and ISV-mono, the stereogenic centers at C1 and C11 adopt an *R*,*R* configuration.

The superposition of the two polymorphs reveals clear conformational differences (Fig. 2). The main distinction lies in the orientation of the 4-(thiazol-4-yl)benzonitrile fragment, which is rotated by approximately 180°. Differences are also evident in the torsion angles: in the orthorhombic form, the torsion angles are −81.6 (2)° (C1—C11—C13—S1) and −37.3 (2)° (C2—C1—C11—C13), whereas in the monoclinic form the corresponding torsion angles are −118.4 (1) and −58.5 (2)°, respectively. Additionally, the dihedral angle between the triazole ring and the 2,5-difluorophenyl ring is 40.14 (8)° in ISV-ortho and 67.6 (1)° in ISV-mono.

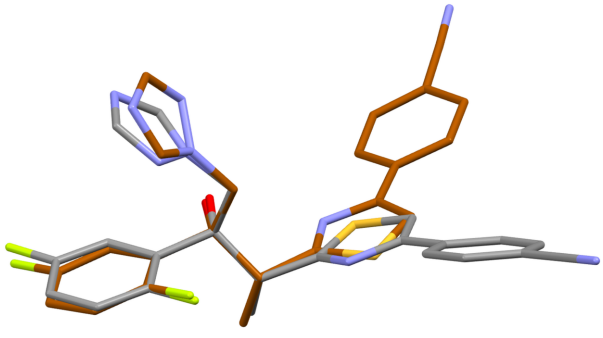

Figure 2
Overlay of the title molecule (ISV-ortho) and the monoclinic polymorph (ISV-mono) with carbon atoms shown in brown.

Table 1
Hydrogen-bond geometry (Å, °).

D—H···*A*	*D*—H	H···*A*	*D*···*A*	*D*—H···*A*
O1—H1···N3^{i}	0.83 (2)	1.99 (3)	2.7889 (16)	164 (3)
C4—H4···N4^{ii}	0.95	2.65	3.277 (2)	124
C11—H11···F1	1.00	2.24	2.9815 (17)	130
C11—H11···N2^{iii}	1.00	2.51	3.317 (2)	138
C12—H12*B*···N5^{iv}	0.98	2.53	3.403 (2)	149

Symmetry codes: (i) $-x, y-\frac{1}{2}, -z+\frac{3}{2}$; (ii) $-x+1, y+\frac{1}{2}, -z+\frac{3}{2}$; (iii) $-x+1, y-\frac{1}{2}, -z+\frac{3}{2}$; (iv) $-x+\frac{3}{2}, -y+1, z+\frac{1}{2}$.

3. Supramolecular features

The monoclinic polymorph of isavuconazole features only C—H···*X* (*X* =N/O/F) hydrogen bonds along with interactions involving π-electrons, such as C—H···π and aromatic π–π stacking interactions (Voronin *et al.*, 2021). A quantum topology analysis revealed that the strongest individual intermolecular interaction in pure ISV-mono does not exceed 11 kJ mol^{-1}. This was taken to indicate a tendency of the API to exhibit amorphization or polymorphism due to the absence of persistent packing motifs (Voronin *et al.*, 2016, 2021).

In this study, we compare the supramolecular architectures of both polymorphs of ISV based on the analysis of interactions energies using the pairwise model implemented in *CrystalExplorer* (Spackman *et al.*, 2021).

In the crystal structure of the orthorhombic form of ISV, the most important O1—H1···N3 hydrogen bond forms a mono-periodic chain substructure running along the crystallographic

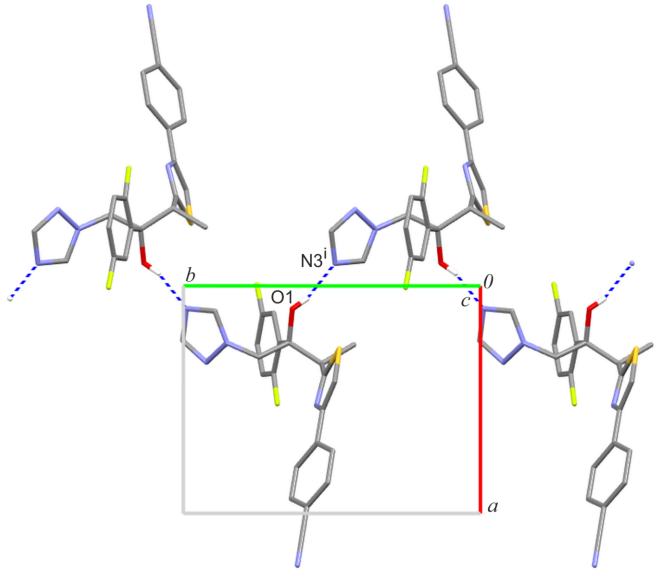

Figure 3
A part of the crystal structure of ISV-ortho showing a mono-periodic chain motif running along the *b*-axis direction. Hydrogen bonds are drawn as dashed lines, and for the sake of clarity, the H atoms bonded to C atoms have been omitted. Symmetry code: (i) $-x, y-\frac{1}{2}, -z+\frac{3}{2}$.

Table 2
Interaction energies (kJ mol^{-1}) for the cluster of molecules with a radius of 3.8 Å for ISV-ortho and ISV-mono.

N is the number of molecular pairs. *R* is the distance (Å) between molecular centroids. E_{tot} is the total energy and E_{ele} is the electrostatic (k = 1.057), E_{pol} is the polarization (k = 0.740), E_{dis} is the dispersion (k = 0.871) and E_{rep} is the repulsion (k = 0.618) component.

N	*R*	kE_{ele}	kE_{pol}	kE_{dis}	kE_{rep}	E_{tot}
ISV-ortho						
2	10.15	−66.8	−13.8	−24.8	47.7	−57.8
2	15.18	−3.8	−1.0	−2.4	0.0	−7.1
2	8.95	−8.0	−1.6	−18.6	10.3	−18.0
2	11.06	−1.1	−1.3	−16.4	7.5	−11.2
2	14.04	−3.2	−0.4	−5.0	0.0	−8.5
2	8.38	−13.4	−2.4	−36.5	16.1	−36.3
2	6.79	−15.1	−3.3	−45.3	23.7	−40.1
2	12.06	−11.2	−2.4	−18.4	0.0	−32.0
2	11.70	−1.3	−0.1	−1.7	0.0	−3.0
ISV-mono						
2	9.75	2.1	−2.1	−34.3	14.4	−19.9
2	5.83	−26.1	−5.7	−70.9	42.8	−59.9
2	8.98	−9.6	−2.4	−26.1	9.0	−29.3
2	11.96	−4.5	−0.7	−5.9	2.3	−8.9
2	10.73	−2.0	−1.0	−13.3	5.1	−11.4
2	9.6	−23.1	−4.1	−24.0	19.6	−31.8
2	12.33	−0.7	−3.4	−17.9	0.0	−22.0
2	14.74	−2.2	−1.0	−2.9	0.0	−6.1

b-axis direction (Table 1, Fig. 3). This interaction is the strongest with a total energy estimated as −57.80 kJ mol^{-1} and the largest contribution arising from Coulombic forces (–66.8 kJ mol^{-1}; Table 2). Three additional C—H···N interactions propagate these chains into a tri-periodic supramolecular network (Fig. 4). Among them, the molecular pair connected by C4—H4···N4 and C11—H11···N2 exhibits the second highest total energy (–40.10 kJ mol^{-1}) with a significant dispersive contribution (–45.3 kJ mol^{-1}), likely due to supporting close contacts between the (difluoro)phenyl ring and the thiazole group. Dispersion effects are also significant for molecular pairs involving contacts between triazole and benzene rings (–36.5 kJ mol^{-1}). The C12—H12*B*···N5 interaction leads to the formation of another sub-chain motif with a total pairwise energy of −32.0 kJ mol^{-1}.

In the crystal structure of the monoclinic form of ISV, the hydroxyl group participates in an intramolecular O—H···N hydrogen bond, thus only the C—H donors contribute to intermolecular interactions, supported by aromatic contacts.

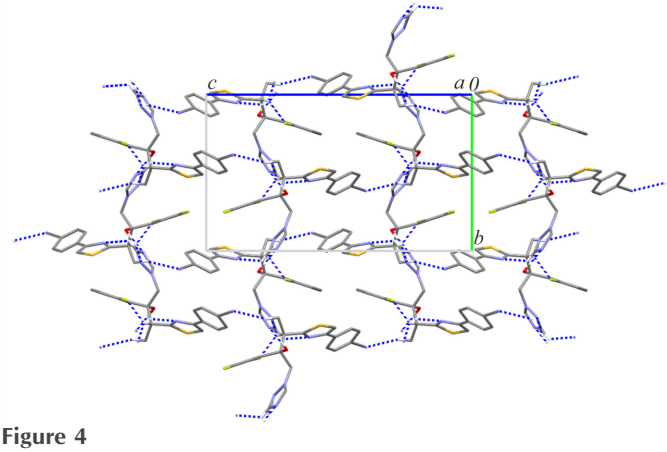

Figure 4
Crystal packing of ISV-ortho showing the formation of a tri-periodic supramolecular network.

The most significant total energies of molecular pairs are summarized in Table 2. It is seen that the highest total pairwise energies are comparable in both polymorphs; however, the interactions responsible for them are completely different. Furthermore, the electrostatic-to-dispersive contribution ratio differs: 25:75 for the monoclinic and 42:58 for the orthorhombic form. This clearly demonstrates that the monoclinic polymorph is dominated by non-directional dispersion interactions, whereas the orthorhombic polymorph shows an increased contribution from Coulombic forces.

4. Hirshfeld surface analysis

Hirshfeld surface analysis (Spackman & McKinnon, 2002; Spackman & Jayatilaka, 2009) was performed using *CrystalExplorer* (Spackman *et al.*, 2021) to visualize and quantify intermolecular interactions in both polymorphs of isavuconazole. As shown in the breakdown diagram (Fig. 5), the major contributions to the Hirshfeld surface in both forms arise from H···H, N···H/H···N, and C···H/H···C contacts. The dominant share of H···H contacts is comparable between the two forms, whereas the proportions of N···H/H···N and C···H/H···C contacts appear complementary. Comparison of 2D fingerprint plots reveals that the main differences originate from N···H/H···N interactions. In the ISV-ortho form, these contacts appear as sharp, long spikes (shorter distances), while in the ISV-mono form, they are much shorter and less pronounced (longer distances). The contribution of F···H/H···F contacts is also higher in the orthorhombic form (14.4%) compared with the monoclinic one (8%). The S···H/H···S interactions show the opposite trend, contributing 3% in ISV-ortho *versus* 5.9% in ISV-mono, likely due to conformational differences that allow additional close contacts with the thiazole ring in ISV-mono. In ISV-ortho, the smaller contribution of S···H interactions seem to be compensated by

S···C contacts. Each of the other contact types contributes less than 10% in both forms.

5. Database survey

A search of the Cambridge Structural Database (CSD version 5.46, November 2024, Groom *et al.*, 2016) revealed four structures of isavuconazole (Voronin *et al.*, 2021): an anhydrous monoclinic form (GALJUC), a monohydrate form (GALJIQ), and two salts with phosphoric acid (GALJOW) and *p*-toluenesulfonic acid (GALJEM).

6. Synthesis and crystallization

The isavuconazole (purity 98%) used in this study was purchased from BLD Pharmatech GmbH (Germany). A pure crystalline form of isavuconazole was obtained unexpectedly from cocrystallization of the drug with pyrazinedicarboxylic acid; all substances (0.05 mmol) were used with a fixed stoichiometric ratio of 1:1, dissolved in ethanol (3 ml EtOH) and the mixture was heated to 346 K.

7. Refinement

Crystal data, data collection and structure refinement details are summarized in Table 3. All hydrogen atoms bonded to carbon atoms were placed geometrically and refined as riding, with U_{iso}(H) = 1.2 U_{eq}(C) for the methylene, methine and aromatic groups or U_{iso}(H) = 1.5 U_{eq}(C) for the methyl group. The hydrogen atom of the hydroxyl group was found in a difference-Fourier map.

Table 3
Experimental details.

Crystal data	
Chemical formula	$C_{22}H_{17}F_2N_5OS$
M_r	437.46
Crystal system, space group	Orthorhombic, $P2_12_12_1$
Temperature (K)	100
a, b, c (Å)	8.9485 (1), 11.6975 (1), 19.8730 (1)
V (Å^3)	2080.21 (3)
Z	4
Radiation type	Cu $K\alpha$
μ (mm^{-1})	1.75
Crystal size (mm)	0.22 × 0.20 × 0.05
Data collection	
Diffractometer	Rigaku XtaLAB Synergy, Dualflex, HyPix
Absorption correction	Gaussian (*CrysAlis PRO*; Rigaku OD, 2024)
T_{min}, T_{max}	0.228, 1.000
No. of measured, independent and observed [$I > 2\sigma(I)$] reflections	32125, 4184, 4132
R_{int}	0.028
(sin $\theta/\lambda)_{max}$ (Å^{-1})	0.633
Refinement	
$R[F^2 > 2\sigma(F^2)]$, $wR(F^2)$, S	0.021, 0.055, 1.03
No. of reflections	4184
No. of parameters	285
H-atom treatment	H atoms treated by a mixture of independent and constrained refinement
$\Delta\rho_{max}$, $\Delta\rho_{min}$ (e Å^{-3})	0.21, −0.19
Absolute structure	Flack x determined using 1711 quotients $[(I^+)-(I^-)]/[(I^+)+(I^-)]$ (Parsons *et al.*, 2013)
Absolute structure parameter	0.002 (4)

Computer programs: *CrysAlis PRO* (Rigaku OD, 2024), *SHELXT* (Sheldrick, 2015*a*), *SHELXL2019/3* (Sheldrick, 2015*b*), *Mercury* (Macrae *et al.*, 2020), *PLATON* (Spek, 2020) and *publCIF* (Westrip, 2010).

8. Pairwise model energies and their energy frameworks

Pairwise model energies (Turner *et al.*, 2014) were estimated and visualized (Turner *et al.*, 2015; Mackenzie *et al.*, 2017) between molecules within a cluster with a radius of 3.8 Å, using *CrystalExplorer* software (Spackman *et al.*, 2021). The computational approach uses a B3LYP/6-31G(d,p) molecular wave function calculated for the respective molecular arrangement in the crystal. The total interaction energy between any nearest-neighbour molecular pairs was estimated in terms of four components: electrostatic, polarization, dispersion and exchange–repulsion, with scale factors (k) of 1.057, 0.740, 0.871 and 0.618, respectively.

Acknowledgements

The financial support from University of Łodz Doctoral School of Exact and Natural Sciences is gratefully acknowledged.

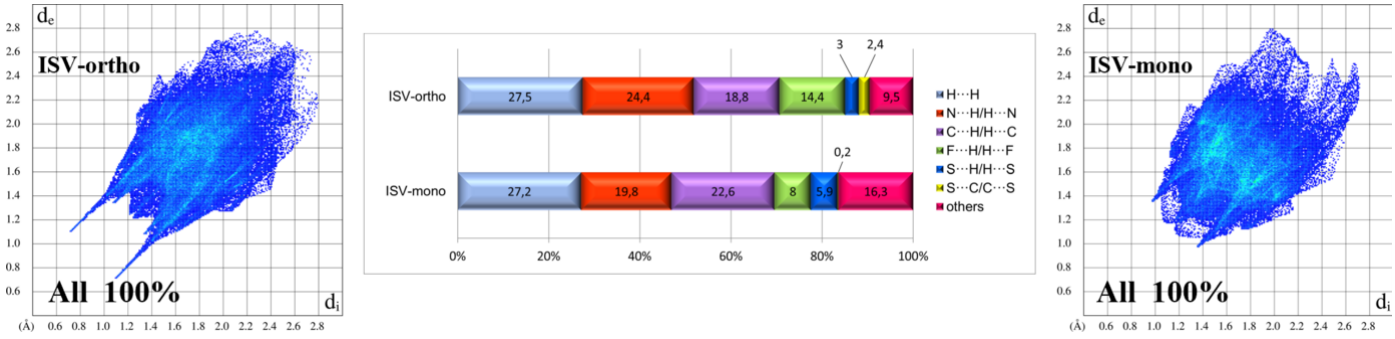

Figure 5
Hirshfeld surface contact contributions and two-dimensional fingerprint plots for ISV-ortho (left) and ISV-mono (right). The d_i and d_e values are the closest internal and external distances (in Å) from given points on the Hirshfeld surface.

References

Groom, C. R., Bruno, I. J., Lightfoot, M. P. & Ward, S. C. (2016). *Acta Cryst.* B**72**, 171–179.

Hussain, M., Qadri, T., Hussain, Z., Saeed, A., Channar, P. A., Shehzadi, S. A. & Malik, A. (2019). *Heliyon* **5**, e02812.

Lewis, J. S. II, Wiederhold, N. P., Hakki, M. & Thompson, G. R. III (2022). *Antimicrob. Agents Chemother.* **66**, e00177–22.

Li, J., Ren, G. Y., Zhang, Y., Yang, M. Y. & Ma, H. X. (2019). *Polyhedron* **157**, 163–169.

Mackenzie, C. F., Spackman, P. R., Jayatilaka, D. & Spackman, M. A. (2017). *IUCrJ* **4**, 575–587.

Macrae, C. F., Sovago, I., Cottrell, S. J., Galek, P. T. A., McCabe, P., Pidcock, E., Platings, M., Shields, G. P., Stevens, J. S., Towler, M. & Wood, P. A. (2020). *J. Appl. Cryst.* **53**, 226–235.

Miceli, M. H. & Kauffman, C. A. (2015). *Clin. Infect. Dis.* **61**, 1558–1565.

Parsons, S., Flack, H. D. & Wagner, T. (2013). *Acta Cryst.* B**69**, 249–259.

Raman, A. P. S., Aslam, M., Awasthi, A., Ansari, A., Jain, P., Lal, K., Bahadur, I., Singh, P. & Kumari, K. (2025). *Mol. Divers.* **29**, 899–964.

Rigaku OD (2024). *CrysAlis PRO*. Rigaku Corporation, Yarnton, England.

Salma, U., Ahmad, S., Zafer Alam, M. & Khan, S. A. (2024). *J. Mol. Struct.* **1301**, 137240.

Sheldrick, G. M. (2015*a*). *Acta Cryst.* A**71**, 3–8.

Sheldrick, G. M. (2015*b*). *Acta Cryst.* C**71**, 3–8.

Shirley, M. & Scott, L. J. (2016). *Drugs* **76**, 1647–1657.

Slaihim, M. M., Al-Suede, F. S. R., Khairuddean, M., Khadeer Ahamed, M. B. & Shah Abdul Majid, A. M. (2019). *J. Mol. Struct.* **1196**, 78–87.

Spackman, M. A. & Jayatilaka, D. (2009). *CrystEngComm* **11**, 19–32.

Spackman, M. A. & McKinnon, J. J. (2002). *CrystEngComm* **4**, 378–392.

Spackman, P. R., Turner, M. J., McKinnon, J. J., Wolff, S. K., Grimwood, D. J., Jayatilaka, D. & Spackman, M. A. (2021). *J. Appl. Cryst.* **54**, 1006–1011.

Spek, A. L. (2020). *Acta Cryst.* E**76**, 1–11.

Turner, M. J., Grabowsky, S., Jayatilaka, D. & Spackman, M. A. (2014). *J. Phys. Chem. Lett.* **5**, 4249–4255.

Turner, M. J., Thomas, S. P., Shi, M. W., Jayatilaka, D. & Spackman, M. A. (2015). *Chem. Commun.* **51**, 3735–3738.

Voronin, A. P., Perlovich, G. L. & Vener, M. V. (2016). *Comput. Theor. Chem.* **1092**, 1–11.

Voronin, A. P., Vasilev, N. A., Surov, A. O., Churakov, A. V. & Perlovich, G. L. (2021). *CrystEngComm* **23**, 8513–8526.

Westrip, S. P. (2010). *J. Appl. Cryst.* **43**, 920–925.

supporting information

Acta Cryst. (2025). E**81**, 1018-1022 [https://doi.org/10.1107/S2056989025008886]

An orthorhombic polymorph of isavuconazole

Anna Ben and Lilianna Chęcińska

Computing details

4-{2-[(2*R*,3*R*)-3-(2,5-Difluorophenyl)-3-hydroxy-4-(1,2,4-triazol-1-yl)butan-2-yl]-1,3-thiazol-4-yl}benzonitrile

Crystal data

$C_{22}H_{17}F_2N_5OS$
$M_r = 437.46$
Orthorhombic, $P2_12_12_1$
$a = 8.9485$ (1) Å
$b = 11.6975$ (1) Å
$c = 19.8730$ (1) Å
$V = 2080.21$ (3) Å^3
$Z = 4$
$F(000) = 904$
$D_x = 1.397$ Mg m^{-3}
Cu $K\alpha$ radiation, $\lambda = 1.54184$ Å
Cell parameters from 28179 reflections
$\theta = 4.4$–$77.0°$
$\mu = 1.75$ mm^{-1}
$T = 100$ K
Plate, colourless
0.22 × 0.20 × 0.05 mm

Data collection

Rigaku XtaLAB Synergy, Dualflex, HyPix diffractometer
Radiation source: micro-focus sealed X-ray tube, PhotonJet (Cu) X-ray Source
Mirror monochromator
Detector resolution: 10.0000 pixels mm^{-1}
ω scans
Absorption correction: gaussian (CrysAlisPro; Rigaku OD, 2024)
$T_{min} = 0.228$, $T_{max} = 1.000$
32125 measured reflections
4184 independent reflections
4132 reflections with $I > 2\sigma(I)$
$R_{int} = 0.028$
$\theta_{max} = 77.3°$, $\theta_{min} = 4.4°$
$h = -10 \rightarrow 10$
$k = -11 \rightarrow 14$
$l = -24 \rightarrow 25$

Refinement

Refinement on F^2
Least-squares matrix: full
$R[F^2 > 2\sigma(F^2)] = 0.021$
$wR(F^2) = 0.055$
$S = 1.03$
4184 reflections
285 parameters
0 restraints
Primary atom site location: structure-invariant direct methods
Hydrogen site location: mixed
H atoms treated by a mixture of independent and constrained refinement
$w = 1/[\sigma^2(F_o^2) + (0.030P)^2 + 0.3775P]$ where $P = (F_o^2 + 2F_c^2)/3$
$(\Delta/\sigma)_{max} = 0.001$
$\Delta\rho_{max} = 0.21$ e Å^{-3}
$\Delta\rho_{min} = -0.19$ e Å^{-3}
Absolute structure: Flack *x* determined using 1711 quotients $[(I^+)-(I^-)]/[(I^+)+(I^-)]$ (Parsons *et al.*, 2013)
Absolute structure parameter: 0.002 (4)

Special details

Geometry. All esds (except the esd in the dihedral angle between two l.s. planes) are estimated using the full covariance matrix. The cell esds are taken into account individually in the estimation of esds in distances, angles and torsion angles; correlations between esds in cell parameters are only used when they are defined by crystal symmetry. An approximate (isotropic) treatment of cell esds is used for estimating esds involving l.s. planes.

Fractional atomic coordinates and isotropic or equivalent isotropic displacement parameters (Å²)

	x	*y*	*z*	U_{iso}*/U_{eq}
S1	0.27613 (4)	0.47460 (4)	0.57074 (2)	0.03016 (10)
F1	0.51741 (10)	0.68366 (8)	0.79865 (5)	0.0253 (2)
F2	−0.00623 (12)	0.75217 (9)	0.92935 (5)	0.0362 (2)
O1	0.10049 (12)	0.63322 (9)	0.69664 (5)	0.0192 (2)
N1	0.25015 (13)	0.85359 (10)	0.70417 (6)	0.0178 (2)
N2	0.33567 (15)	0.92245 (11)	0.74385 (7)	0.0219 (3)
N3	0.09947 (14)	0.98951 (11)	0.73679 (6)	0.0224 (3)
N4	0.52605 (14)	0.55185 (11)	0.61439 (6)	0.0208 (3)
N5	1.22751 (19)	0.61588 (15)	0.39819 (8)	0.0391 (4)
C1	0.24879 (16)	0.64444 (12)	0.72044 (7)	0.0174 (3)
C2	0.31189 (16)	0.74593 (12)	0.67995 (7)	0.0189 (3)
H2A	0.422088	0.747449	0.684257	0.023*
H2B	0.286951	0.736175	0.631761	0.023*
C3	0.11079 (17)	0.89399 (12)	0.70097 (8)	0.0202 (3)
H3	0.031324	0.859480	0.676635	0.024*
C4	0.24030 (17)	1.00243 (13)	0.76200 (8)	0.0228 (3)
H4	0.267423	1.064314	0.790447	0.027*
C5	0.25190 (16)	0.67557 (11)	0.79592 (7)	0.0183 (3)
C6	0.38393 (17)	0.69634 (13)	0.83090 (8)	0.0210 (3)
C7	0.3890 (2)	0.73257 (13)	0.89697 (8)	0.0258 (3)
H7	0.482322	0.744423	0.918691	0.031*
C8	0.2569 (2)	0.75139 (13)	0.93113 (7)	0.0284 (3)
H8	0.256705	0.776037	0.976678	0.034*
C9	0.12582 (19)	0.73321 (14)	0.89692 (8)	0.0255 (3)
C10	0.11984 (17)	0.69603 (13)	0.83093 (8)	0.0210 (3)
H10	0.026052	0.684490	0.809584	0.025*
C11	0.34188 (16)	0.53393 (12)	0.70649 (7)	0.0196 (3)
H11	0.434223	0.539147	0.734658	0.023*
C12	0.25850 (19)	0.42638 (13)	0.72888 (8)	0.0257 (3)
H12A	0.169462	0.415987	0.700824	0.038*
H12B	0.228474	0.434422	0.776063	0.038*
H12C	0.324116	0.359800	0.724093	0.038*
C13	0.39205 (17)	0.52523 (13)	0.63439 (7)	0.0208 (3)
C14	0.42004 (19)	0.49034 (15)	0.51479 (8)	0.0292 (3)
H14	0.414034	0.473052	0.468164	0.035*
C15	0.54393 (18)	0.53089 (13)	0.54615 (7)	0.0234 (3)
C16	0.69074 (18)	0.54990 (13)	0.51454 (8)	0.0244 (3)
C17	0.7979 (2)	0.61881 (15)	0.54546 (8)	0.0306 (4)
H17	0.775707	0.654112	0.587329	0.037*

C18	0.9363 (2)	0.63651 (17)	0.51599 (9)	0.0341 (4)
H18	1.008092	0.684119	0.537319	0.041*
C19	0.9696 (2)	0.58388 (15)	0.45471 (8)	0.0291 (4)
C20	0.86455 (19)	0.51375 (14)	0.42361 (8)	0.0275 (3)
H20	0.887849	0.477219	0.382228	0.033*
C21	0.7261 (2)	0.49738 (13)	0.45314 (7)	0.0262 (3)
H21	0.654342	0.450069	0.431590	0.031*
C22	1.1127 (2)	0.60168 (16)	0.42323 (9)	0.0326 (4)
H1	0.056 (3)	0.584 (2)	0.7187 (12)	0.040 (6)*

Atomic displacement parameters (Å²)

	U^{11}	U^{22}	U^{33}	U^{12}	U^{13}	U^{23}
S1	0.02487 (18)	0.0387 (2)	0.02694 (18)	0.00058 (17)	−0.00362 (15)	−0.01020 (16)
F1	0.0180 (4)	0.0266 (5)	0.0312 (5)	−0.0017 (4)	−0.0013 (4)	−0.0015 (4)
F2	0.0370 (5)	0.0408 (5)	0.0306 (5)	0.0009 (5)	0.0150 (4)	−0.0053 (4)
O1	0.0168 (5)	0.0170 (5)	0.0238 (5)	−0.0015 (4)	−0.0019 (4)	0.0011 (4)
N1	0.0182 (6)	0.0153 (5)	0.0198 (5)	−0.0005 (5)	0.0003 (5)	0.0009 (4)
N2	0.0202 (6)	0.0190 (6)	0.0266 (6)	−0.0021 (5)	−0.0020 (5)	−0.0023 (5)
N3	0.0204 (6)	0.0182 (6)	0.0286 (6)	0.0016 (5)	−0.0009 (5)	−0.0011 (5)
N4	0.0245 (6)	0.0174 (6)	0.0204 (6)	0.0047 (5)	0.0004 (5)	−0.0008 (5)
N5	0.0384 (9)	0.0498 (9)	0.0293 (7)	0.0012 (8)	0.0074 (7)	0.0022 (7)
C1	0.0165 (7)	0.0157 (6)	0.0199 (6)	0.0003 (5)	−0.0001 (5)	−0.0004 (5)
C2	0.0191 (7)	0.0163 (7)	0.0214 (6)	0.0016 (5)	0.0021 (5)	0.0002 (6)
C3	0.0188 (7)	0.0179 (7)	0.0238 (7)	0.0000 (6)	−0.0009 (6)	0.0007 (6)
C4	0.0222 (7)	0.0184 (7)	0.0279 (7)	−0.0009 (6)	−0.0022 (6)	−0.0028 (5)
C5	0.0212 (7)	0.0134 (6)	0.0205 (6)	−0.0005 (5)	0.0000 (6)	0.0013 (5)
C6	0.0215 (7)	0.0166 (7)	0.0249 (7)	−0.0003 (6)	0.0010 (6)	0.0010 (6)
C7	0.0310 (8)	0.0207 (8)	0.0257 (7)	−0.0034 (7)	−0.0069 (7)	0.0000 (6)
C8	0.0422 (9)	0.0229 (7)	0.0202 (6)	−0.0021 (7)	0.0006 (7)	−0.0019 (6)
C9	0.0298 (8)	0.0217 (8)	0.0251 (7)	0.0008 (6)	0.0085 (6)	−0.0002 (6)
C10	0.0219 (7)	0.0171 (7)	0.0240 (7)	−0.0009 (6)	0.0017 (6)	0.0007 (6)
C11	0.0197 (6)	0.0172 (7)	0.0218 (7)	0.0022 (6)	−0.0012 (5)	−0.0008 (6)
C12	0.0277 (8)	0.0166 (7)	0.0327 (8)	0.0036 (6)	0.0021 (7)	0.0026 (6)
C13	0.0218 (7)	0.0166 (7)	0.0239 (7)	0.0039 (6)	−0.0022 (6)	−0.0030 (6)
C14	0.0313 (8)	0.0332 (9)	0.0231 (7)	0.0064 (7)	−0.0030 (6)	−0.0064 (7)
C15	0.0303 (8)	0.0197 (7)	0.0203 (7)	0.0068 (6)	−0.0001 (6)	−0.0016 (6)
C16	0.0307 (8)	0.0226 (7)	0.0200 (7)	0.0077 (6)	0.0011 (6)	0.0023 (6)
C17	0.0348 (9)	0.0330 (9)	0.0240 (7)	0.0021 (7)	0.0039 (7)	−0.0056 (7)
C18	0.0341 (9)	0.0384 (10)	0.0297 (8)	−0.0004 (8)	0.0037 (7)	−0.0041 (7)
C19	0.0337 (9)	0.0300 (8)	0.0237 (7)	0.0079 (7)	0.0050 (7)	0.0049 (6)
C20	0.0382 (9)	0.0248 (7)	0.0195 (7)	0.0110 (7)	0.0023 (6)	0.0024 (6)
C21	0.0358 (8)	0.0223 (7)	0.0203 (6)	0.0062 (7)	−0.0007 (6)	0.0007 (5)
C22	0.0378 (9)	0.0362 (9)	0.0238 (7)	0.0083 (8)	0.0034 (7)	0.0019 (7)

Geometric parameters (Å, º)

S1—C14	1.7112 (17)	C7—H7	0.9500
S1—C13	1.7398 (15)	C8—C9	1.372 (2)
F1—C6	1.3636 (18)	C8—H8	0.9500
F2—C9	1.3642 (18)	C9—C10	1.383 (2)
O1—C1	1.4149 (17)	C10—H10	0.9500
O1—H1	0.83 (3)	C11—C13	1.505 (2)
N1—C3	1.335 (2)	C11—C12	1.529 (2)
N1—N2	1.3625 (18)	C11—H11	1.0000
N1—C2	1.4570 (18)	C12—H12A	0.9800
N2—C4	1.317 (2)	C12—H12B	0.9800
N3—C3	1.329 (2)	C12—H12C	0.9800
N3—C4	1.3645 (19)	C14—C15	1.357 (2)
N4—C13	1.301 (2)	C14—H14	0.9500
N4—C15	1.3875 (19)	C15—C16	1.473 (2)
N5—C22	1.154 (2)	C16—C17	1.396 (2)
C1—C2	1.5412 (19)	C16—C21	1.402 (2)
C1—C5	1.5438 (19)	C17—C18	1.385 (3)
C1—C11	1.5627 (19)	C17—H17	0.9500
C2—H2A	0.9900	C18—C19	1.397 (2)
C2—H2B	0.9900	C18—H18	0.9500
C3—H3	0.9500	C19—C20	1.392 (3)
C4—H4	0.9500	C19—C22	1.441 (2)
C5—C10	1.392 (2)	C20—C21	1.384 (2)
C5—C6	1.392 (2)	C20—H20	0.9500
C6—C7	1.380 (2)	C21—H21	0.9500
C7—C8	1.381 (2)		
C14—S1—C13	89.26 (7)	C9—C10—H10	120.2
C1—O1—H1	110.0 (16)	C5—C10—H10	120.2
C3—N1—N2	110.06 (12)	C13—C11—C12	111.54 (12)
C3—N1—C2	130.12 (12)	C13—C11—C1	112.57 (12)
N2—N1—C2	119.29 (12)	C12—C11—C1	111.65 (11)
C4—N2—N1	102.39 (12)	C13—C11—H11	106.9
C3—N3—C4	102.67 (12)	C12—C11—H11	106.9
C13—N4—C15	111.26 (13)	C1—C11—H11	106.9
O1—C1—C2	103.92 (11)	C11—C12—H12A	109.5
O1—C1—C5	111.32 (11)	C11—C12—H12B	109.5
C2—C1—C5	108.60 (11)	H12A—C12—H12B	109.5
O1—C1—C11	111.34 (11)	C11—C12—H12C	109.5
C2—C1—C11	110.44 (11)	H12A—C12—H12C	109.5
C5—C1—C11	110.97 (11)	H12B—C12—H12C	109.5
N1—C2—C1	110.76 (11)	N4—C13—C11	123.34 (13)
N1—C2—H2A	109.5	N4—C13—S1	114.13 (11)
C1—C2—H2A	109.5	C11—C13—S1	122.51 (11)
N1—C2—H2B	109.5	C15—C14—S1	110.73 (11)
C1—C2—H2B	109.5	C15—C14—H14	124.6

H2A—C2—H2B	108.1	S1—C14—H14	124.6
N3—C3—N1	110.08 (13)	C14—C15—N4	114.60 (14)
N3—C3—H3	125.0	C14—C15—C16	125.84 (14)
N1—C3—H3	125.0	N4—C15—C16	119.53 (14)
N2—C4—N3	114.79 (13)	C17—C16—C21	118.74 (15)
N2—C4—H4	122.6	C17—C16—C15	120.84 (14)
N3—C4—H4	122.6	C21—C16—C15	120.41 (15)
C10—C5—C6	116.15 (13)	C18—C17—C16	120.97 (15)
C10—C5—C1	120.72 (13)	C18—C17—H17	119.5
C6—C5—C1	122.80 (13)	C16—C17—H17	119.5
F1—C6—C7	116.84 (14)	C17—C18—C19	119.56 (17)
F1—C6—C5	119.31 (13)	C17—C18—H18	120.2
C7—C6—C5	123.82 (15)	C19—C18—H18	120.2
C6—C7—C8	119.22 (15)	C20—C19—C18	120.19 (16)
C6—C7—H7	120.4	C20—C19—C22	119.51 (15)
C8—C7—H7	120.4	C18—C19—C22	120.30 (17)
C9—C8—C7	117.61 (13)	C21—C20—C19	119.83 (15)
C9—C8—H8	121.2	C21—C20—H20	120.1
C7—C8—H8	121.2	C19—C20—H20	120.1
F2—C9—C8	118.75 (14)	C20—C21—C16	120.70 (15)
F2—C9—C10	117.76 (15)	C20—C21—H21	119.7
C8—C9—C10	123.49 (15)	C16—C21—H21	119.7
C9—C10—C5	119.69 (14)	N5—C22—C19	179.8 (2)

C3—N1—N2—C4	−0.52 (15)	C2—C1—C11—C13	−37.30 (16)
C2—N1—N2—C4	−172.96 (12)	C5—C1—C11—C13	−157.78 (12)
C3—N1—C2—C1	−67.54 (18)	O1—C1—C11—C12	−48.73 (15)
N2—N1—C2—C1	103.15 (14)	C2—C1—C11—C12	−163.64 (12)
O1—C1—C2—N1	73.99 (13)	C5—C1—C11—C12	75.87 (15)
C5—C1—C2—N1	−44.61 (15)	C15—N4—C13—C11	177.28 (13)
C11—C1—C2—N1	−166.50 (11)	C15—N4—C13—S1	−1.04 (16)
C4—N3—C3—N1	−0.67 (16)	C12—C11—C13—N4	−133.40 (15)
N2—N1—C3—N3	0.79 (16)	C1—C11—C13—N4	100.19 (16)
C2—N1—C3—N3	172.15 (13)	C12—C11—C13—S1	44.79 (17)
N1—N2—C4—N3	0.10 (17)	C1—C11—C13—S1	−81.62 (15)
C3—N3—C4—N2	0.35 (18)	C14—S1—C13—N4	0.40 (13)
O1—C1—C5—C10	−3.97 (18)	C14—S1—C13—C11	−177.93 (13)
C2—C1—C5—C10	109.85 (14)	C13—S1—C14—C15	0.37 (14)
C11—C1—C5—C10	−128.58 (14)	S1—C14—C15—N4	−1.05 (19)
O1—C1—C5—C6	−177.17 (12)	S1—C14—C15—C16	177.01 (12)
C2—C1—C5—C6	−63.35 (17)	C13—N4—C15—C14	1.36 (19)
C11—C1—C5—C6	58.23 (17)	C13—N4—C15—C16	−176.83 (13)
C10—C5—C6—F1	−176.72 (13)	C14—C15—C16—C17	162.90 (17)
C1—C5—C6—F1	−3.2 (2)	N4—C15—C16—C17	−19.1 (2)
C10—C5—C6—C7	1.5 (2)	C14—C15—C16—C21	−18.1 (2)
C1—C5—C6—C7	174.96 (14)	N4—C15—C16—C21	159.86 (14)
F1—C6—C7—C8	177.32 (13)	C21—C16—C17—C18	0.7 (2)
C5—C6—C7—C8	−0.9 (2)	C15—C16—C17—C18	179.76 (16)

C6—C7—C8—C9	−0.3 (2)	C16—C17—C18—C19	−0.5 (3)
C7—C8—C9—F2	−179.42 (14)	C17—C18—C19—C20	−0.3 (3)
C7—C8—C9—C10	0.8 (2)	C17—C18—C19—C22	179.77 (17)
F2—C9—C10—C5	−179.98 (13)	C18—C19—C20—C21	0.8 (2)
C8—C9—C10—C5	−0.2 (2)	C22—C19—C20—C21	−179.20 (15)
C6—C5—C10—C9	−0.9 (2)	C19—C20—C21—C16	−0.6 (2)
C1—C5—C10—C9	−174.52 (13)	C17—C16—C21—C20	−0.2 (2)
O1—C1—C11—C13	77.62 (14)	C15—C16—C21—C20	−179.18 (14)

Hydrogen-bond geometry (Å, º)

D—H···*A*	*D*—H	H···*A*	*D*···*A*	*D*—H···*A*
O1—H1···N3^{i}	0.83 (2)	1.99 (3)	2.7889 (16)	164 (3)
C4—H4···N4^{ii}	0.95	2.65	3.277 (2)	124
C11—H11···F1	1.00	2.24	2.9815 (17)	130
C11—H11···N2^{iii}	1.00	2.51	3.317 (2)	138
C12—H12*B*···N5^{iv}	0.98	2.53	3.403 (2)	149

Symmetry codes: (i) −*x*, *y*−1/2, −*z*+3/2; (ii) −*x*+1, *y*+1/2, −*z*+3/2; (iii) −*x*+1, *y*−1/2, −*z*+3/2; (iv) −*x*+3/2, −*y*+1, *z*+1/2.